Numerical Investigation of Nucleated Bubbles around a Heated Square Obstacle using Thermal Hybrid Lattice Boltzmann Method

Salaheddine Channouf[1][a], Mohammed Jami[1][b] and Ahmed Mezrhab[1][c]

[1] *Mechanical and energetic laboratory, First Mohamed university, faculty of sciences, Oujda, Morocco*

Keywords: Boiling phenomenon, nucleated bubbles, lattice Boltzmann method, 2-order Runge-Kutta finite difference scheme, heat transfer, phase-change.

Abstract: The phenomenon of boiling has become one of the challenges of the LB community in recent years, as it is frequently used in industry and deals with a complex natural phenomenon. For this purpose, we have developed a computational code that allows us to simulate this phenomenon around a square obstacle of variable length in a rectangular cavity. We aim to study the behaviour of nucleated bubbles which appear around this obstacle due to its heat exchange with the liquid. The pseudopotential multi-relaxation time lattice Boltzmann method MRT-LBM proposed by (Li, 2013) is used as a solver of the fluid flows combined with the 2-order Runge-Kutta finite difference scheme for modelling the phase change from a liquid to a vapour phase *(Zhao,2018)* and the temperature field.

1 INTRODUCTION

Lattice Boltzmann method (LBM) has become a precision and efficient tool for simulating hydro-thermodynamic phenomena because its simplicity of implementation and insertion of boundaries. This method contains 2 main steps represented by a distribution function denoted $f_i(\boldsymbol{x},t)$ which presents a set of particles having precise velocities in a regular mesh called lattice Boltzmann and follows their movements in phase space. These two steps describe the collision and streaming of particles over time on the lattice (Meng, 2014) and allow to have a simple algorithm to calculate the macroscopic variables as density, velocity components, temperature, etc. In this paper, the collision and streaming steps are represented in momentum space, this space aims to shift each macroscopic quantity towards the equilibrium by the multi-relaxation time (MRT) collision operator model (Krüger, 2017) as opposed to the simple relaxation time operator known as the BGK operator model (Andries, 2002) which is used to relax the distribution function around the equilibrium distribution function. The MRT model is used due to its reliability and high stability. In our work, the pseudopotential MRT-LBM approach (Shan,2014) is adopted. This is the famous model of the LB community for the simulation of a multiphase flow thanks to its simplicity to obtain the separation of the phases without the need to track at each step time the interface between the phases. This model allows to successfully simulate several numerical problems in multiphases such as wettability, condensation, boiling, collapsing and rising bubbles, etc.

In the present work, this model is combined with the celebrate Runge-Kutta finite difference scheme (Zhao, 2018, Zheng, 2018) to simulate the thermal behavior of liquid chosen at saturated temperature during phase change around a heated obstacle with a variable characteristic length D.

2 METHODOLODY

The hybrid model proposed in this work is described by the following equation

$$f_i^{*}(\boldsymbol{x},t) = f_i(\boldsymbol{x},t) - \boldsymbol{M^{-1}\Lambda M}\big(f_i(\boldsymbol{x},t) - f_i^{eq}(\boldsymbol{x},t)\big) + \delta t\boldsymbol{MF} \quad (1)$$

[a] https://orcid.org/0000-0002-8538-5629
[b] https://orcid.org/0000-0002-5356-4729
[c] https://orcid.org/0000-0001-6013-7496

Channouf, S., Jami, M. and Mezrhab, A.
Numerical Investigation of Nucleated Bubbles around a Heated Square Obstacle using Thermal Hybrid Lattice Boltzmann Method.
DOI: 10.5220/0010730400003101
In *Proceedings of the 2nd International Conference on Big Data, Modelling and Machine Learning (BML 2021)*, pages 171-174
ISBN: 978-989-758-559-3

The term in the left hand represents the post-collision distribution function which can be calculated with the previous distribution function $f_i(\boldsymbol{x}, t)$ by subtracting its disturbance around the equilibrium distribution function relaxing by nine relaxation times given by the relaxation matrix $\boldsymbol{\Lambda}$ and by adding the forcing term $\boldsymbol{F}$. The parameters $\boldsymbol{M}$ and $\boldsymbol{M}^{-1}$ describe the transformation matrix and its inverse from the phase space to the momentum space.

The 2-order Runge-Kutta finite difference scheme is used as a solver of energy equation to simulate the liquid-vapor phase-change transformation as (Zhao, 2018, Zheng, 2018)

$$\frac{dT}{dt} = -\mathbf{v}.\boldsymbol{\nabla}T - \frac{T}{\rho c_v}\left(\frac{\partial P_{EOS}}{\partial t}\right)_\rho \boldsymbol{\nabla}.\mathbf{v} + \frac{1}{\rho c_v}\boldsymbol{\nabla}.(\lambda\boldsymbol{\nabla}T) \qquad (2)$$

P_{EOS} is the pressure according to equation of state proposed by Peng-Robinson (Yuan, 2006) which is calculated from the pseudopotential function, λ is the thermal conductivity and c_v is the specific heat coefficient $\mathbf{v}$ is the macroscopic velocity of flows and ρ is the macroscopic density. These macroscopic parameters can be calculated as follows

$$\rho = \sum_i f_i \; ; \; \rho\mathbf{u} = \sum_i f_i c_i \qquad (3)$$

$\boldsymbol{c_i}$ is the lattice speed in i^th direction.

3 VALIDATION MODEL

Figures 1 and 2 show the validation of our code using the work of Zheng et al. (Zheng, 2018) to check its accuracy and its efficiency. For this purpose, a thermohydrodynamic effect is investigated to simulate the evaporation behavior of a heated liquid droplet placed in the center of a cavity and surrounded by a saturated vapor by implementing the periodic boundary for all cavity walls in which the thermal conductivity is set to be constant $\lambda = 1$ which allows to neglect the convective effect.

From Figure 2, the results show a reducing of initial radius of droplet over time δt, this reduction is described by the square rate of change of the radius with a negative slope line. However, the vector field shown in Figure 1 shows the direction of the loss of liquid mass caused by the transformation of the liquid into vapor. The same remarks are made from the reference work. Therefore, our numerical results show a strong corresponding with those reported by Zheng et al. (Zheng, 2018).

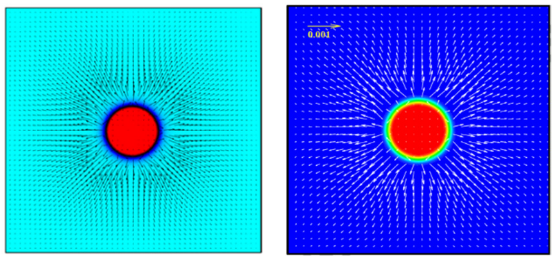

(a) Our result (b) Zheng et al. (Zheng, 2018)

Figure 1: Comparative results with reference (Zheng, 2018)

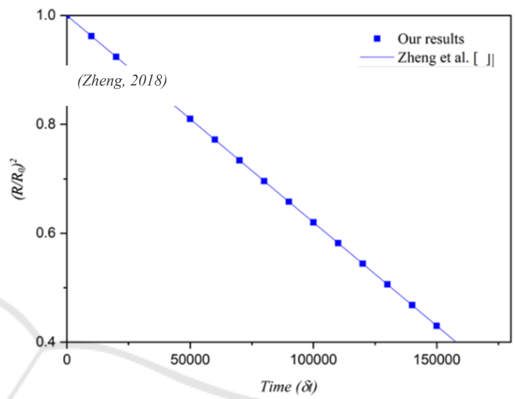

Figure 2: Square rate change of radius over time δt in comparison with reference (Zheng, 2018).

4 RESULTS AND DISCUSSIONS

4.1 Presentation of the Computational Problem

Figure 3 shows the computational domain of a saturated liquid confined in a rectangular cavity of height H and length L in which a heated square obstacle at temperature $T_h = 1.16T_{c_r}$ is placed halfway between the vertical walls at a distance of $H/6$ from the bottom wall. The obstacle has a height h and a variable characteristic length D. In our simulation, the critical temperature is set to be $T_{c_r} = 0.07292$. For the fluid flow, the periodic boundaries are selected for both right and left vertical walls. The bounce-back boundaries are adopted for the bottom wall, while the outflow boundary is applied on the top wall. For the obstacle faces, the no-slip boundaries are selected. Their density value is adjusted to be in a non-wetting phase. All computational domain is set at saturated temperature T_{sat}.

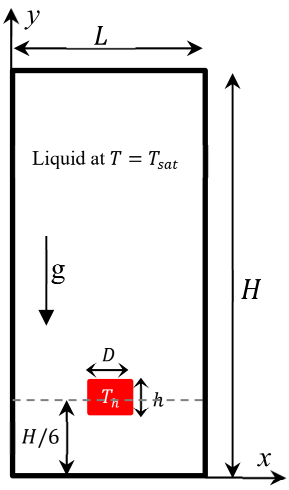

Figure 3: Illustration of the computational problem.

4.2 Formation Pattern of Nucleated Bubble around the Obstacle

Figure 4 illustrated the density behavior of both liquid and vapor during phase change caused by the heated obstacle. It can be seen that the nucleated bubble formed around the obstacle grows progressively over time until its volume becomes important, then, it moves upward due to the buoyant force.

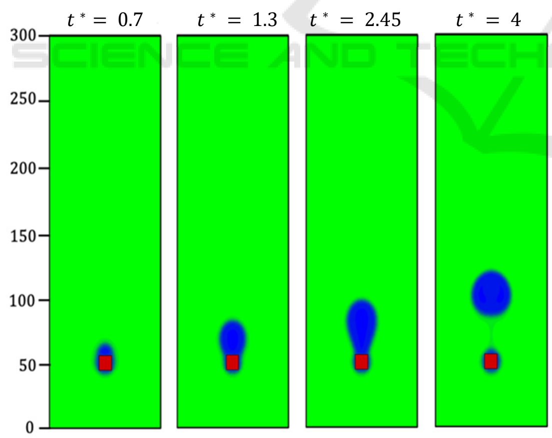

Figure 4: Steps of the nucleated bubble formation around the heated obstacle.

Figure 5 describes the velocity at three different positions near to the obstacle at time $t^* = 3.66$ corresponding to the final step of formation of nucleated bubble. At $y = H/6$, the velocity is zero on the obstacle and tends to increase in the surrounding area. However, it remains weak due to friction with the solid. At the obstacle-liquid interface ($y = H/6 + h/2$), the velocity increases but it keeps the same form. finally, at $y = H/6 + h$, an intense peak due to the buoyancy effect during nucleation is noted.

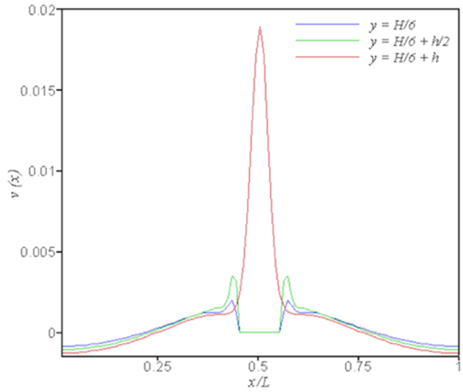

Figure 5: The velocity component in y-direction at different positions.

The heat flux exchanged between the obstacle and the liquid is illustrated in Figure 6 at three different positions and at $t^* = 3.66$. This heat leads to the formation of the nucleated bubbles. For $y = H/6$, the exchange flux is greater at the vertical solid-liquid interfaces then it decreases to be zero when moving away from these interfaces. At position $y = H/6 + h/2$, the exchanged flux behaves in the same way as in the first case but it is reduced. For the last position, a decrease in flux at the center of the curve is noted. This is due to the flux transferred to the bubbles.

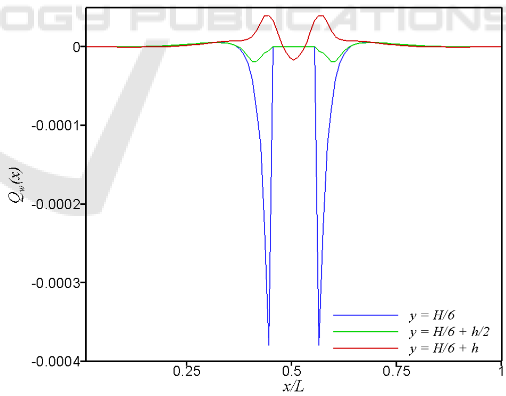

Figure 6: The exchange heat flux between liquid and heated obstacle at different positions.

4.3 Effect of Variation of Characteristic Length D on Nucleation

In this part, we adjusting the characteristic length D to study its impact on the nucleated bubble for-mation. The same parameters of fluid flows and temperature field are chosen as the previous part.

Figure 7 gives the behavior of the velocity component in the y direction for three different values of D and for the position $y = H/6 + h$. We notice that the velocity decreases with the increase of D. Indeed, when D increases, the number of nucleated bubbles increases then they merge to give a large bubble which is more slowed down by the liquid.

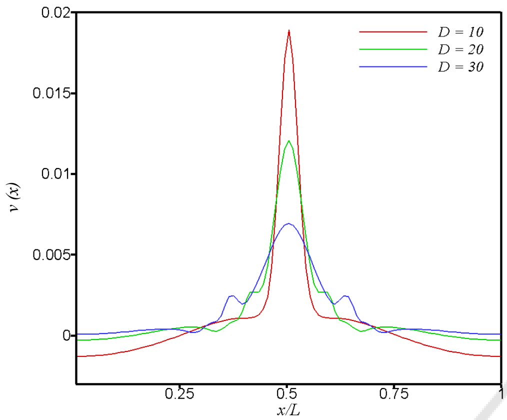

Figure 7: The velocity component in y-direction by varying the length D of the obstacle at y = H/6+h.

Figure 8 shows the heat flux exchanged between the upper face of the solid and the liquid to give more details on the formation of nucleated bubbles around the obstacle. For this purpose, the heat flux exchanged is studied for three different values of the characteristic length D. The curves show that the increase in the characteristic length leads to an increase in heat flux at the right and left sides of the obstacle. Moreover, in the middle of the cavity in the x direction, the heat flux form changes with D and indicates that the heat transferred to the liquid is important for small bubbles than for large bubbles.

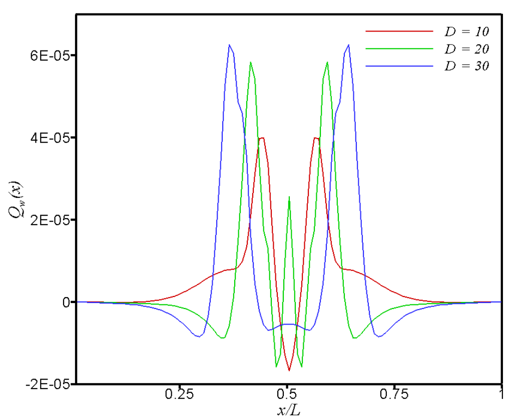

Figure 8: The exchange heat flux between liquid and heated obstacle by varying the length D of the obstacle at y = H/6+h.

5 CONCLUSIONS

In the light of this work, we can draw the following conclusions:

- When the characteristic length D increases, the heat exchange between the solid and the liquid increases at the vertical faces of the obstacle. However, this flux decreases in the area of nucleated bubbles.
- The large bubble formed by the nucleated bubbles is all the more slowed down as its volume is important.

These results allow us to make the right choice of the characteristic length D that gives a compatible boiling shape. In future work, 3D will investigate and validate that with experiment by applying this method to the study of phase change materials.

REFERENCES

Li, Q., Luo, K. H., & Li, X. J. 2013. Lattice Boltzmann modeling of multiphase flows at large density ratio with an improved pseudopotential model. Physical Review E, 87(5), 053301.

Zhao, W., Zhang, Y., Xu, B., Shang, W., & Jiang, S. 2018. Pseudopotential multiple-relaxation-time lattice Boltzmann simulation of vapor condensation on vertical subcooled walls. arXiv preprint arXiv:1808.04973.

Meng, J., & Zhang, Y. 2014. Diffuse reflection boundary condition for high-order lattice Boltzmann models with streaming–collision mechanism. Journal of Computational Physics, 258, 601-612.

Krüger, T., Kusumaatmaja, H., Kuzmin, A., Shardt, O., Silva, G., & Viggen, E. M. 2017. MRT and TRT Collision Operators. In the Lattice Boltzmann Method (pp. 407-431). Springer, Cham.

Andries, P., Aoki, K., & Perthame, B. 2002. A consistent BGK-type model for gas mixtures. Journal of Statistical Physics, 106(5), 993-1018.

Shan, X., & Chen, H. 1993. Lattice Boltzmann model for simulating flows with multiple phases and components. Physical review E, 47(3), 1815.

Zheng, S., Eimann, F., Fieback, T., Xie, G., & Gross, U., 2018. Numerical investigation of convective dropwise condensation flow by a hybrid thermal lattice Boltzmann method. Applied Thermal Engineering, 145, 590-602.

Yuan, P., & Schaefer, L. (2006). Equations of state in a lattice Boltzmann model. Physics of Fluids, 18(4), 042101.

Chen, L., Kang, Q., Mu, Y., He, Y. L., & Tao, W. Q. (2014). A critical review of the pseudopotential multiphase lattice Boltzmann model: Methods and applications. International journal of heat and mass transfer, 76, 210-236.